

Lipid Biochemical and Biophysical Changes in Rat Spermatozoa During Isolation and Functional Activation *In Vitro*¹

Running title: SPERM LIPIDS AFTER SPERM ISOLATION AND ACTIVATION

Gerardo M. Oresti², Daniel A. Peñalva, Jessica M. Luquez, Silvia S. Antollini, and Marta I. Aveldaño

Instituto de Investigaciones Bioquímicas de Bahía Blanca, Consejo Nacional de Investigaciones Científicas y Técnicas (CONICET) y Universidad Nacional del Sur (UNS), Bahía Blanca, Argentina.

¹Supported by grants from: Agencia Nacional de Promoción Científica y Tecnológica (ANPCyT, PICT2013-1356 and PICT2013-2533), Consejo Nacional de Investigaciones Científicas y Técnicas (CONICET, PIP-2012) and Universidad Nacional del Sur (UNS, PGI-24/B169).

²Correspondence: Gerardo Martín Oresti, Instituto de Investigaciones Bioquímicas de Bahía Blanca (INIBIBB), Centro Científico Tecnológico Bahía Blanca, CONICET, La Carrindanga KM 7, CC 857, 8000 Bahía Blanca, Argentina. Phone (54) (291) 4861666, ext. 138; fax (54) (291) 4861200; e-mail: gmoresti@criba.edu.ar

ABSTRACT

In spermatozoa isolated from rat epididymis, lipids are differentially modified after *in vitro* induction of capacitation (Cap) and the acrosomal reaction (AR). This study uses Laurdan fluorescence generalized polarization values (GPv) to evaluate the effect of lipid changes occurring after isolation and functional activation on sperm membrane biophysical properties. In gametes isolated in the presence of a divalent cation chelator no lipid changes occurred and the GPv were the lowest recorded, indicating maximal membrane lipid mobility. In sperm isolated as rapidly and gently as possible in the absence of chelator, part of the sphingomyelins (SM) were converted into ceramides (Cer), giving rise to higher GPv. In samples incubated as controls for Cap and AR, unchanged cholesterol and reduced glycerophospholipid (GPL) levels were accompanied by the accumulation of free fatty acids (FFA), leading to even higher GPv. After completion of Cap the GPv returned to lower levels as result of the spermatozoa losing part of their cholesterol and FFA. Cap samples became relatively enriched in PUFA-containing plasmalogens, since hydrolysis affected phosphatidyl rather than plasmenyl GPL subclasses. The highest Cer/SM ratio and the highest GPv were found after completion of AR, induced by A23187. The degree of SM→Cer conversion among samples, including controls, correlated with the extent of AR. FFA and Cer augmented GPv when added to liposomes prepared from the membrane lipid of intact sperm. Our results underscore the importance of hydrolytic changes that affect sperm lipids, especially the decisive lipid SM/Cer pair, not only after inducing sperm functional changes such as Cap and AR, but also under control conditions.

Summary sentence: Ceramides and free fatty acids formed during isolation, and functional activation *in vitro* promote biophysical alterations in rat spermatozoa membrane.

Keywords: acrosomal reaction; capacitation; ceramides; free fatty acids; generalized polarization; membrane lipid order

INTRODUCTION

In rat spermatozoa, glycerophospholipids (GPL) have been known for decades to be rich in species containing long-chain polyunsaturated fatty acids (PUFA), especially 22:5n-6 and 20:4n-6 [1]. In these gametes, choline and ethanolamine GPL (CGP, EGP) are made up of high proportions of plasmalogens, of which plasmenylcholine in particular is rich in an atypical PUFA, 22:4n-9 [2]. Because rat spermatozoa typically have a tiny head compared with their long and voluminous tail, a considerable proportion of these PUFA-rich GPL belong to the latter. The sphingomyelin (SM) of rat sperm is also unique as it contains, N-linked to the sphingosine base, very-long-chain (VLC) PUFA of the n-6 series, in the form of nonhydroxy VLCPUFA (n-V) and 2-hydroxy VLCPUFA (h-V) [3], of which (n- and h-) 28:4n-6, 30:5n-6 and 32:5n-6 are the most abundant [4,5]. These SM species are exclusive to the sperm heads [6].

When isolating rat spermatozoa from the epididymal *cauda* for lipid analytical purposes it is useful to include EDTA in the isolation media right from the initial stages in order to control the activity of divalent cation-dependent phosphohydrolases. This strategy, previously used to prevent the conversion of SM into ceramide (Cer), revealed a further peculiarity of rat sperm lipid, namely the endogenous presence of significant amounts of h-V Cer [4]. The explanation for this intriguing feature lies in the fact that unlike the head-located n-V SM or h-V SM, these h-V Cer species are found exclusively in the tails [7].

The uniqueness of rat sperm lipid fatty acids facilitates the direct observation of hydrolytic reactions that affect them to different extents under two conditions linked to important functional states of spermatozoa: capacitation (Cap) and the acrosomal reaction (AR). Thus, after Cap is induced by sperm incubation in a bicarbonate-, albumin- and calcium-containing medium, in addition to the canonical efflux of free cholesterol [8], a decrease in the level of GPL and a concomitant displacement of free fatty acids (FFA) from gametes to the medium occurs [9]. After the calcium-dependent AR is induced in capacitated sperm by the addition of a calcium ionophore (A23187), significant amounts of Cer are produced from the original SM [9].

Since lipid compositional changes are primary mechanisms by which membrane phase behavior is modified, they may be expected to result in measurable alterations in sperm membrane biophysical properties. In the present study, our aim was to find possible correlations between biochemical and biophysical changes that modify sperm membrane lipids after isolation, incubation and functional activation. Lipid composition was assessed using classic chromatographic techniques. The biophysical state was evaluated by means of Laurdan fluorescence spectroscopy in liposomes and native membranes, a widely used technique for studying bilayer structure and lipid phase changes [10] owing to its high sensitivity to the presence and mobility of water molecules trapped within the lipid bilayer [11]. Polarity alterations in the microenvironment of Laurdan in bilayers give rise to variations in its fluorescence excitation and emission spectra, quantifiable by calculating the Laurdan generalized polarization (GP) values. Changes in this parameter indicate shifts in the degree of lipid order. The lower the GP values, the lower the structural order of lipids in model or biological membranes. The present results highlight the dynamic nature of the changes affecting sperm lipids after procedures commonly employed to experimentally imitate physiological changes undergone by spermatozoa, pointing to the importance of the control conditions in determining such changes.

MATERIAL AND METHODS

Rat spermatozoa were obtained from Wistar rats aged 3-4 months, maintained and sacrificed in strict accordance with the National Institutes of Health Guide for the Care and Use of Laboratory Animals and following the guidelines approved by the Institutional Committee for the Care of Laboratory Animals (CICUAE) of the Universidad Nacional del Sur, Argentina. Epididymal cauda were excised, freed of their surrounding tissues and transferred to small dishes. A few incisions were made in each epididymis with a scalpel and the organs were maintained for 15 minutes at 34°C [12] to allow for sperm release and diffusion into one of the following aqueous media: either phosphate buffered saline (PBS) containing 2.5 mM EDTA (Control 1, here abbreviated as C1) or Biggers-Whitten-Whittingham (BWW) medium (Control 2, here abbreviated as C2).

The C1 control samples were prepared to generate a sperm suspension in which the presence of the chelator prevented divalent cation-dependent hydrolytic reactions from affecting lipids [6]. The second controls (C2) were freshly isolated samples, suspended in the described BWW medium with no

chelator but containing glucose (5.5 mM), pyruvate (0.3 mM) and lactate (21 mM). The C2 suspensions served as the source of spermatozoa for the following samples, which were incubated using the same BWW as the common medium.

Incubated spermatozoa. After isolation, sperm suspensions prepared as indicated for C2 samples were diluted to 10×10^6 cells / ml with BWW medium and separated into three containers. Each one was then diluted to contain 5×10^6 cells / ml by adding an equal volume of BWW medium, containing either no additions (C3 samples) or appropriate concentrations of the reagents required to reach capacitation (Cap) or the acrosomal reaction (AR). This cell dilution was carried out in order to avoid physical stress factors such as centrifugation and pipetting, as either of them decreases significantly the motility of rat spermatozoa [13]. The sperm suspensions were incubated under 5% CO₂ atmosphere for 5.5 hours at 37°C in BWW medium containing: i) no additions (C3 samples), ii) 25 mM NaHCO₃, 1.7 mM CaCl₂, and 0.4% fatty acid-free bovine serum albumin (Cap samples), and iii) the same components as the latter with the addition of the calcium ionophore A23187 (to reach a 10 μM concentration) half an hour prior to completing the incubations (AR samples).

Aliquots from sperm suspensions obtained after the described isolation (C1, C2) and incubation (C3, Cap, AR) procedures were used to determine the sperm numbers, using a Neubauer hemocytometer, and to evaluate sperm viability, protein tyrosine phosphorylation and acrosomal status (Fig. 1). The bulk of sperm suspensions were then subjected to a gentle centrifugation (5 min at 400 x g) and the gametes were washed by careful re-suspension in PBS, then collected by a second brief centrifugation (3 min at 200 x g). Lipid extracts were prepared [14] from the cells. Aliquots from these extracts were taken to determine the total phospholipid (PL) content in the samples by measuring the amount of lipid phosphorus [15].

Sperm Viability, Protein Phosphorylation, and Acrosomal Status

Immediately prior to lipid extraction, aliquots from all sperm suspensions were stained for 15 minutes with Hoechst 33342 (5 μM, final concentration) to locate spermatozoa by nuclei staining and propidium iodide (PI) (0.5 μM, final concentration) to identify gametes with damaged membranes. Spermatozoa were observed and counted under phase contrast / epifluorescence illumination and fluorescence microscopy was carried out using appropriate filters in a Nikon Eclipse E-600 microscope. After counting 200 sperm from each sample, the percentage of dead spermatozoa was estimated from the ratio between Hoechst positive (all sperm) and PI positive (dead sperm) nuclei.

Phosphorylation of sperm proteins in tyrosine residues was used as an indicator of the capacitation state [16]. Aliquots containing 15×10^6 gametes from each experimental condition were pelleted and washed in 1 ml of PBS, resuspended in sample buffer [17] with no mercaptoethanol and boiled for 5 minutes. After centrifuging at 5,000g for 3 minutes, the supernatants were recovered and boiled in the presence of 5% 2-mercaptoethanol for 5 minutes. Then, aliquots equivalent to 6.5×10^6 cells were subjected to SDS-PAGE on 8% polyacrylamide gels and transferred to a polyvinylidene fluoride membrane (Immobilon P, Millipore, Bedford, MA). After blocking overnight with 3% of skim milk in TBS-T buffer (20 mM Tris-HCl, pH 7.4, 100 mM NaCl and 0.1% Tween 20), the blots were analyzed for levels of tyrosine-phosphorylated proteins using a specific anti-phosphotyrosine monoclonal antibody [PY20] (HRP-conjugated, Abcam-16389) (1:2500), enhanced chemiluminescence detection using an ECL detection kit (Thermo Scientific Pierce) and exposure to an x-ray-sensitive film. The same immunoblots were probed with antibodies against tubulin for loading control.

The acrosomal status of sperm cells was assessed using the Coomassie brilliant blue G-250 dye method of Larson and Miller [18] as described [19]. Spermatozoa were fixed with 4% paraformaldehyde at pH 7.4 for 10 min, centrifuged, washed with 0.1M ammonium acetate at pH 9.0, and taken up from the pellets in 100 μl of 0.1M ammonium acetate. Aliquots smeared on glass microscope slides were air-dried and the slides were stained for 2 min at room temperature with freshly prepared Coomassie stain (0.22% Coomassie Blue G-250, 50% methanol, 10% glacial acetic acid, 40% water). After washing and air-drying, the slides were covered with a cover slip over Permount mounting solution and observed under a bright field microscope at 1000X magnification. The heads of spermatozoa with an intact acrosome stained blue over their dorsal and ventral surfaces, while those of acrosome-reacted sperm stained only over the ventral surface. The number of spermatozoa that had undergone the AR was then calculated as a percentage of the 200 spermatozoa from each of the experimental conditions.

Lipid Separation and Analysis

In order to compare the *qualitative* profile of the rat sperm lipids (polar and neutral) in the 5 experimental conditions of our study namely the two non-incubated controls (C1-C2) and the three incubated samples (C3-Cap-AR), a single mono-dimensional TLC plate was first prepared using a combination of solvents capable of showing as many of the rat sperm lipid classes as possible (Fig. 2A). After determining the number of cells and the amount of total phospholipids (PL) as lipid phosphorus per sample, the amount of total PL per fixed number of cells decreased in the order C1, C2, C3, Cap, AR (Fig. 2 B). By the same token, the number of cells per fixed amount of PL increased in the same order. As shown in Fig. 2A, the same amount of lipid phosphorus (10 µg) per condition was taken from lipid extracts prepared from each of the 5 conditions and spotted onto an HP-TLC silica gel plate (Merck). The following solvents were then employed: firstly, chloroform : methanol : acetic acid : water (50:37.5:3.5:2 by vol) [20] was run up to approximately the middle of the plates to resolve the PL classes; then, after drying the plates, diethyl ether was run, allowing it to overpass the solvent front by 1 cm, in order to concentrate the neutral lipids into a single sharp band; and finally hexane:ether (80:20 by vol) was run up to the top of the plates to resolve the neutral lipids. A plate containing lipid standards was developed simultaneously for lipid identification.

The main phospholipid classes shown in Fig. 2B were quantified after similar separations, except that the mentioned solvent mixture [20] was allowed to run up to the top of the TLC plates. The bands containing these PL classes were transferred to tubes, followed by phosphorus analysis of spots [15]. The data in Fig. 2B and in Figures 3-5 show amounts of lipids, or lipid fatty acids, expressed per billion (10^9) cells.

Isolation of neutral and polar lipid classes for further analysis was performed by preparative TLC using 20 x 20 cm plates covered with 500 µm-thick layers of silica gel 60, essentially as described in previous work [7]. Briefly, the neutral lipids were first separated from the total polar lipids. To this end, most of each lipid extract was spotted under N₂, the solvent mixture chloroform : methanol : aqueous ammonia (90:10:2 by vol) was allowed to run up to the middle of the plates to move up the (n-V and h-V) ceramides, and then hexane/ether (80:20, by vol) was allowed to reach the top of the same plates to separate free fatty acids (FFA) and free cholesterol from other neutral lipids. The total polar lipids were then recovered from the origin of these plates, eluted from the support, and used for further separations. Portions of these eluates were taken to obtain the (diradyl) choline and ethanolamine glycerophospholipids (CGP and EGP, respectively) and the sphingomyelins (species with non-hydroxy and 2-hydroxy fatty acids).

The CGP and EGP glycerophospholipid classes were isolated by two-dimensional TLC [15] to separate them into their main phosphatidyl- and plasmeryl- subclasses (plasmalogens). The spots containing the CGP and EGP were scraped from the plates followed by elution and quantification by phosphorus analysis in eluate aliquots. After drying, other aliquots of CGP and EGP were briefly (1 min) exposed to a small volume of 0.5 N HCl in acetonitrile [2], rapidly evaporating this solvent and resolving the lipid products by TLC using chloroform : methanol : water (65:25:4, by vol). By virtue of the sensitivity to acid of the vinyl-ether bond present in plasmalogens, their fatty aldehydes were released and their corresponding (2-acyl) lysoPC and lysoPE widely separated from the unaffected phosphatidylcholine (PC) and phosphatidylethanolamine (PE). After TLC separation, these main subclasses were recovered for further analysis (phosphorus, fatty acids).

For the preparative isolation of SM, a generous fraction of the total polar lipid fraction was spotted onto TLC plates and chloroform : methanol : acetic acid : 0.15 M NaCl (50:25:8:2.5 by vol) was used as solvent. The SM together with the previously obtained Cer were subjected to a mild alkali treatment followed by a second TLC to free them from any potential co-migrating lipid with ester-bound fatty acids [21].

With the exception of the data shown in Fig. 2, in which lipid classes were located with iodine vapors, lipids were located under UV light after spraying the plates with dichlorofluorescein, scraped from the plates and collected into tubes for elution. This was achieved by three successive extractions of the silica support by vigorously mixing it with water : methanol : chloroform (1:5:5, by vol.), centrifuging, collecting the solvents, and partitioning the resulting solvent mixtures with four volumes of water to recover the lipids in the organic phases.

After elution, cholesterol was measured using a commercial kit, other neutral lipids (ceramides, FFA, diglycerides, triglycerides) were quantified by analysis of their fatty acid constituents and the phospholipids by both phosphorus and fatty acid analysis. The latter was performed after converting the lipids to fatty acid methyl esters (FAME), followed by gas-chromatography (GC), using the

conditions and instrumentation described in previous work [4,5]. Briefly, after adding appropriate internal standards, transesterification was performed with 0.5N H₂SO₄ in N₂-saturated anhydrous methanol by keeping the samples overnight at 45°C under N₂ in screw-capped tubes. The resulting FAME were routinely purified by TLC on pre-cleaned silica Gel G plates using hexane : ether (95:5, by vol). In the case of FAME derived from SM and Cer, hexane/ether (80:20, v/v) up to the middle of the plates was used to recover the 2-hydroxy FAME, followed by hexane/ether (95:5, v/v) up to near the top to obtain the nonhydroxy FAME. After elution and drying, the former were converted into O-TMS derivatives and the latter analyzed directly by GC as with the rest of the fatty acids.

Biophysical Studies

The biophysical modifications associated with the five experimental conditions of this study were followed in liposomes prepared from the total lipid extracted from the gametes and also directly in the sperm cells, by fluorescence spectroscopy. Liposomes were prepared by mixing appropriate aliquots of the lipid extracts and Laurdan (6-dodecanoyl-2-dimethylaminonaphthalene) (Molecular Probes Inc., USA), drying this mixture under a stream of N₂ for 1 h in the dark, resuspending it in HEPES buffer (20 mM HEPES, 150 mM NaCl, and 0.25 mM MgCl₂, pH 7.4) and subjecting it to sonication for 30 min. In all cases the phospholipid:Laurdan mole ratio was 100:1. Each sample was diluted with this same buffer to reach a final lipid concentration of 150 µg/ml in the (5 x 5 mm) quartz cuvettes that were used for measurements.

To assess the effect of increasing amounts of Cer and FFA on GP values, Laurdan-containing liposomes were prepared taking as the base the total polar lipid (PL) obtained from control sperm samples isolated in the presence of EDTA (C1). This PL was separated from neutral lipids by TLC as explained above and then combined with cholesterol and h-V Cer in the proportions typically present in fresh sperm samples. The mixture taken as control contained a PL: cholesterol: h-V Cer mole ratio of 80 : 20: 0.6, to which was added an FFA mixture with a composition resembling that of the FFA produced under C3 conditions (28% 16:0, 36% 18:0 and 36% 18:1) and Cer obtained from pools of spermatozoa incubated under Cap and AR conditions.

To estimate GP values in native membranes, Laurdan was added directly to the five experimental sperm sample conditions. Suspensions containing 1.5x10⁶ rat sperm cells were collected by a rapid centrifugation, re-suspension in 1 mL HEPES buffer mixed with Laurdan (0.2 µM final concentration) and incubation for 20 min at 37 °C. This labeling time was chosen based on our microscopy observations indicating that Laurdan remained located in the plasma membrane between 15 and 30 min, longer times allowing the probe to diffuse into the cells.

Fluorimetric measurements were performed in a SLM model 4800 fluorimeter (SLM Instruments, Urbana, IL) using the vertically polarized light beam from a Hannovia 200 W Hg/Xe arc obtained with a Glan-Thompson polarizer (4 nm excitation and emission slits). Emission spectra were corrected for wavelength-dependent distortions. The temperature was set with a thermostated circulating water bath.

The GP values were calculated according to the expression $exGP: (I_{434}-I_{490})/(I_{434}+I_{490})$, where I₄₃₄ and I₄₉₀ are the emission intensities at the characteristic wavelength of the gel phase (434 nm) and the liquid-crystalline phase (490 nm), respectively. For liposomes, the excitation wavelength was 360 nm. For intact sperm cells, 360 nm and 290 nm were used for direct excitation and Förster resonance energy transfer (FRET) conditions, respectively.

Statistical Analyses

All results are expressed as mean values ± SD from at least 4 independent experiments in the case of compositional data and from at least 3 experiments in the case of GP measurements. Statistical differences between pairs of samples were evaluated by unpaired Student's t tests. Comparisons of more than two groups of samples were evaluated by 1-way analysis of variance (ANOVA) followed by Bonferroni's multiple comparison test. Differences were considered significant at P < 0.01.

RESULTS

Sperm Viability, Capacitation, and Acrosomal Statuses

Spermatozoa in all experimental conditions showed more than 80% viability and conserved their membrane integrity, as determined by the exclusion of propidium iodide (Fig. 1A and 1B).

Intriguingly, significant rates of spontaneous AR were observed in non-capacitated controls (C1, C2 and C3: 7%, 12%, 29%, respectively) and capacitated spermatozoa (Cap, 48%). After incubation of capacitated sperm in the presence of A23187 as an evoker of the AR, most of the gametes had completed the reaction (91%) (Fig. 1C).

Attainment of the capacitated state was indicated by the presence of high levels of protein tyrosine phosphorylation in the 50-120 kDa range, with a pattern resembling that described for mice [16] in Cap and AR samples (Fig. 1D). Although, as expected, the non-incubated controls (C1 and C2) presented low, non-specific levels of protein tyrosine phosphorylation, this was significantly higher in the controls incubated for 5.5 hours in BWW medium (C3) than in the non-incubated controls. Another indication that sperm capacitation had been reached was that more than 90% of the Cap sperm population showed hyperactivation (data not shown).

Lipid Biochemical Changes

The changes affecting the lipid levels (Figs. 2 to 5) and GP values (Fig. 6; see also Figure 8 discussed below) in rat spermatozoa after the five conditions or treatments of this study are presented in the same order: C1 and C2 correspond to non-incubated control sperm samples isolated directly from the epididymis, in the presence of EDTA and in its absence, respectively, while C3, Cap, and AR correspond to spermatozoa isolated as in C2 and then incubated for the same time periods with no additions, or with the additions required to reach capacitation or to complete the acrosomal reaction, respectively.

A qualitative view of the main polar and neutral lipids of rat sperm in these five conditions, obtained after spotting the same amount of lipid phosphorus per spot from the corresponding lipid extracts, is shown in Fig. 2A. A large increase in FFA and lysoPC concentrations as a consequence of incubation was clearly visible in C3, the levels dropping again in Cap and AR samples. A continuous trend of decreasing SM and increasing Cer levels in the order C1→C2→C3→Cap→AR was also apparent. The data in Fig. 2B depict the changes affecting the levels of total PL, CGP, EGP and SM based on phosphorus analysis. The decrease affecting SM was apparently lipid-class selective, as its levels were significantly higher in C1 than in C2, two control situations in which the major CGP and EGP remained virtually unmodified (Fig. 2B). This SM reduction obviously occurred during sperm isolation. Comparison with the C1 and C2 controls show that a further significant reduction in SM levels occurred during incubation in the sperm samples serving as controls (C3) for Cap and AR samples. The drop in SM continued during incubations leading to the latter two states, reaching a maximum after completion of the AR (Fig. 2B).

In agreement with previous work [9], the levels of (diradyl) CGP and EGP levels were higher in C3 than after Cap and AR (Fig. 2B). The fact that rat spermatozoa are rich in plasmalogens [2,7] prompted the question of how much plasmalogen and plasmalogen subclasses contributed to the observed decreases in CGP and EGP. Our results show that both plasmalogens remained virtually unchanged in the three control conditions (Fig. 3) when compared with the corresponding diacyl subclasses. Thus, hydrolysis of the phosphatidyl- (PC and PE), rather than the plasmalogen- subclasses (abbreviated as P-PC and P-PE in Fig. 3), was a main contributor to the decrease in CGP and EGP levels observed in C3 controls, and could also be responsible for the increased levels of FFA, lyso-GPL and DRG generated in these samples (Fig. 3). Levels of phosphatidylcholine, phosphatidylethanolamine and to a lesser extent plasmalogen, were significantly lower after Cap and AR. Comparing plasmalogens, the major plasmalogen decreased more than the minor plasmalogen, the latter remaining virtually unchanged from controls to AR (Fig. 3). Thus, Cap and AR samples became relatively richer in plasmalogens than any of the three controls.

The membrane lipid profile of sperm Cap and AR samples differed from controls not only in lipid (Fig. 3) but also in fatty acid composition (Fig. 4). The molecular species of PC and PE that decreased the most from C1 to AR were those containing 22:5n-6. By contrast, the species of plasmalogens that underwent the least changes under the same conditions were those containing 22:4n-9, a PUFA that is typical of rat sperm plasmalogen (Fig. 4).

FFA levels clearly showed early increases associated with sperm isolation (C2 with respect to C1) and the drastic effect of incubation (C3 with respect to C2). The highest amounts of FFA among all samples was found in C3, where they accounted for as much as 10-15 % of the total lipid mass per cell, on a mole basis.

Lysophospholipids (LPE and LPC) and diglycerides, mostly DAG, showed a similar trend to FFA, although quantitatively lower, again with the maximum amounts per cell being observed in C3, the samples subjected to incubation under control conditions (Fig. 3). In contrast to the apparent instability of phospholipids suggested by the generation of these metabolites, the amount of free cholesterol per cell remained virtually the same for all three (C1, C2, C3) control conditions.

The high levels of FFA and lyso-GPL in the C3 controls reverted to low in the gametes incubated under Cap conditions (Fig. 3). This coincided with the fact that nearly 30% of the total sperm cholesterol had effluxed from Cap samples to the medium, a lipid change that is considered a requisite for mammalian sperm capacitation [8]. As the phospholipid content also decreased from C3 to Cap cells, this result suggests that part of the FFA and lyso-GPL generated in Cap samples was displaced from the gametes to the Ca^{2+} - HCO_3^- -BSA-containing medium. The combination of lipid hydrolysis and efflux resulted in a significant decrease in the lipid content of the cells.

The data in Fig. 3 also show the levels of sphingomyelin (SM) and ceramide (Cer), estimated using the same method of quantitation, GC of their fatty acids, in order to compare them on the same basis. As the total content of SM in samples decreased in the order C1→C2→C3→Cap→AR, the levels of total Cer increased in an almost stoichiometric equivalence in the opposite direction (Fig. 3). The continuous trend of hydrolysis of SM to Cer from C1 to AR resulted in a large change in sperm lipid composition, as the resulting Cer virtually replaced the original SM. These Cer, having practically the same fatty acid composition as the original SM (Fig. 5), were mostly retained by the gametes after completion of AR, indicating that isolated sperm are essentially devoid of endogenous ceramidase activity.

The rat sperm samples obtained in the presence of EDTA (C1) contained a small proportion of Cer with 2-hydroxy VLCPUFA (h-V Cer), but virtually lacked Cer species with nonhydroxy-VLCPUFA (n-V Cer) or saturated Cer (Fig. 5). The amounts of total sperm Cer increased as a result of isolation in C2, as a result of incubation in C3, in response to incubation in a medium that led to capacitation in Cap samples, and as the most important manifestation of the A23187-mediated changes in AR samples (Figs. 3 and 5).

The strong association between SM hydrolysis to Cer and acrosomal exocytosis was sustained by the positive correlation ($r^2=0.98$) observed between the degree of AR (Fig. 1) and the SM/Cer ratio (Fig. 3 and 4), both increasing significantly in the order C1→C2→C3→Cap→AR.

Lipid Biophysical Changes

Protein-free model membranes. Liposomes prepared from total lipid extracts obtained from rat spermatozoa after treatment in each of the five conditions of this study showed that the C1 control samples exhibited the lowest GP values (Fig. 6), indicative of the lowest degree of lipid order in this condition. At 37 °C, the GP increased significantly in C2 and even more so in C3 samples. As these three controls contained nearly the same amount of cholesterol (Fig. 3), this increase may be largely attributed to increasing levels of one or more of the lipid metabolites (namely FFA, lysophospholipids, DRG or Cer) that were produced in the presence of reduced amounts of the original GPL and SM.

In liposomes from Cap spermatozoa, the GP values significantly decreased with respect to those of the corresponding C3 controls (Fig. 6), indicating an increase in lipid mobility or disorder, with a partial restoration of the original condition. Interestingly, even though the GP values were lower in Cap than in C3, they were nevertheless higher than in C1- and C2- derived samples. This may be a consequence of Cap gametes in part having considerably less cholesterol, but also in part having much less FFA, lysoPL or diglycerides than the corresponding C3 controls per cell, especially less FFA (Fig. 3).

Liposomes prepared with the total lipid from AR spermatozoa displayed the highest GP values (Fig. 6). This feature, representative of the highest restriction to lipid mobility, may be largely attributed to the Cer generated at the expense of SM in AR samples, accumulating to the point of overriding the increase in lipid “disorder” that was a feature of Cap samples. The differences among GP values between samples were observed at different temperatures, but were progressively less marked as the temperature decreased, as illustrated when comparing 37 °C and 23 °C in Fig. 6.

Taken together, the results in Fig. 6 and the composition data suggest that the increase in lipid order observed in C3 and AR samples can be attributed mainly to the FFA and Cer accumulated in each case, respectively, these neutral lipids restricting the free mobility of the main GPL components. To test this possibility, increasing proportions of FFA and Cer were added to Laurdan-probed liposomes previously prepared to imitate the endogenous lipid composition of sperm samples. The

combination taken as control contained on a mole basis, 80 % of the total polar lipid (PL) isolated from C1 samples, 20% of cholesterol and 0.6% of h-V Cer (arrow in Fig. 7).

The most negative bar for the GP values in Fig. 7 corresponds to liposomes prepared with only the polar lipid from gametes of the C1 condition. As anticipated, this preparation displayed the highest degree of lipid disorder. When these liposomes included 20% cholesterol, the also predictable lipid ordering influence of this neutral lipid was observed. The GP values increased even further when as little as 0.6% h-V Cer was added to these cholesterol-containing samples. (Fig. 7). This last combination, taken as the reference (arrow), clearly displayed significantly lower GP values than samples that contained added FFA, Cer, or a mixture of both. In other words, increasing proportions of FFA or Cer, resulted in increasing values of GP with respect to a common control condition (Fig. 7).

The consequences of rising concentrations were stronger for Cer than for FFA, as GP values increased to similar extents with 1% of Cer as with 10% of FFA, and were as high with 10% Cer as with 20% FFA. The concurrent presence of 1% FFA and 1% Cer increased the GP values by nearly as much as 10% FFA or 10 % Cer alone, i.e., more than additively. Interestingly, the effects of increasing FFA or Cer levels were non-linear: , increasing the amount from 10% of FFA or 10% Cer (Fig. 7) to 20% caused a slight increase in GP values t in the case of FFA, but a significant reduction in the case of Cer.

Native Sperm Membranes. To gain information about lipid order *in situ* in sperm cells, Laurdan was added directly to the gametes of the five experimental conditions of this study, excited at 360 nm, and the GP values were calculated for each condition. Previous work using Laurdan-probed human spermatozoa at the lipid/probe ratio used here showed that Laurdan remains localized in the plasma membrane, causing no cytotoxicity or decrease in sperm motility [22-24]. Taking the GP value of C1 samples as the reference, the profile of GP variations was similar to that observed in liposomes of the sperm lipid, except that Cap spermatozoa exhibited the lowest GP values, even somewhat lower than those of C1 controls (Fig. 8).

When membrane samples are excited at 290 nm, a property of Laurdan is its ability to act as a Förster resonance energy transfer (FRET) acceptor of the energy from the excited tryptophan molecules of integral membrane proteins, acting as donors. This capacity was used to learn about the physical state of lipid located within Förster distance of proteins in the sperm membrane, i.e., the lipid that closely surrounds such proteins. As expected, this “annular” lipid showed GP values that tended to be higher than those corresponding to the whole membrane, indicating a higher restriction to its mobility than that affecting the bulk lipid (Fig. 8).

Although the increases in GP values were higher for the extracted lipid (Fig. 6) than for intact cells (Fig. 8), both showed the same tendency to significantly raise GP values from C1 to C2 and to raise them sharply from C2 to C3. Compared to the latter, GP values dropped significantly in liposomes and gametes as a result of Cap and increased several fold over Cap values after completion of the AR.

DISCUSSION

The present results show that significant alterations in lipid composition occur during rat sperm isolation, incubation and functional activation, which correlate with consistent changes in the biophysical state of the sperm membrane. The hydrolysis of SM to Cer appears to be one of the earliest and most sensitive lipid biomarkers of the reactivity of the rat acrosome since small but significant SM decreases and concomitant Cer increases were already observed in C2 samples, associated with an also small but significant degree of AR.

The high sensitivity of the rat sperm acrosome during isolation may in part be ascribed to the presence of divalent cations in the surrounding media. The contact of gametes with even small volumes of the Ca²⁺-rich extracellular fluids is unavoidable when they are isolated, as occurs with the excised epididymal tissue in C2. The difference in SM and Cer levels between C1 and C2 samples, manipulated similarly except for the presence of EDTA in the former case, supports this conclusion. The relatively subtle increase in Cer levels in C2 controls was reflected in significantly augmented Laurdan GP values (Fig. 7). Accordingly, in liposomes imitating the composition of C1 spermatozoa (Fig. 8), the *absence* of Cer resulted in significantly lower GP values than when it was present at 0.6% concentration.

The conversion of SM into Cer and the number of acrosome-reacted gametes continued to increase in C3 samples, which served as controls for Cap and AR. The C2 gametes lacked sufficient time and those under C3 conditions lacked an appropriate stimulus enabling them to reach a capacitated state,

since *in vitro* initiation and completion of capacitation are absolutely dependent on extracellular Ca^{2+} and HCO_3^- in addition to a cholesterol-sequestering agent [25]. This $\text{SM} \rightarrow \text{Cer}$ hydrolysis, and this form of spontaneous AR, thus occurred in purportedly non-capacitated spermatozoa. However small, the gametes incubated in C3 conditions showed a detectable level of protein tyrosine phosphorylation, intermediate between that of non-incubated and capacitated samples. This may be attributed in part to the loss and/or dilution of the surface-bound proteins known as “decapacitating factors”, some of which are of epididymal origin, that may have been detached from the sperm surface during the control incubations. Interestingly, two of the four proteins identified in murine spermatozoa as decapacitating factor candidates do interact with lipids: membrane fatty acid binding protein and phosphatidylethanolamine binding protein-1 [26].

Optimal conditions of sperm recovery vary according to the animal species [27]. When isolated from the epididymis, rat spermatozoa are much more vulnerable to suboptimal conditions of centrifugation and pipetting than bull, boar, or ram spermatozoa [13] and also to other physical stress conditions, such as chilling [28] and cryopreservation [29]. All of these factors affect sperm motility, acrosome integrity, or both. Sperm cells that react prematurely (spontaneous AR) are thought to compromise their ability to penetrate the egg vestments [30].

Although from the standpoint of lipid composition we generated a robust intact rat sperm control by including EDTA (C1) in the isolation medium, we do not advocate its use for biological studies. Even though the cell viability was not affected, these sperms presented low motility. Recovery of their original functional potentialities by removing the chelator is possible, although this was not checked, and would require some of the lab manipulations known to adversely affect rat sperm (resuspension by pipetting, washing, centrifugations). These experimental controls were intended to provide a “picture” of how rat sperm lipids would look (biochemically) and behave (biophysically) if they were undisturbed by lipid hydrolyzing enzymes, just as a protease inhibitor is used if the aim is to isolate intact proteins from cells or tissues. They show that in order to obtain a biologically valid control (as is the case of the C2 samples), the additional precaution of keeping sperm contact with epididymal fluids at a minimum is an additional factor to take into account when deciding on the sperm quality/quantity balance required for a given study.

An intriguing collateral observation of this study was that rat sperm from *cauda* epididymis contained small amounts of triacylglycerols (TAG). These lipids were initially thought to arise from contaminating oily droplets or from small membrane-bound structures derived from epididymal tissues or fluids during isolation. However, a closer view showed that a relatively high proportion of caudal gametes (45-50%) contained a faint, small (2-3 μm in size) cytoplasmic droplet (CD) located on their tails, a residual organelle normally absent in ejaculated but present in maturing epididymal spermatozoa. Each of these CDs enclosed a Nile-Red positive (neutral lipid-containing) *lipid droplet* (Supplemental Figure S1; all supplemental figures are available online at www.biolreprod.org). When a fraction containing these CDs was isolated by a procedure based on the fact that the gentle physical shearing forces generated by a discontinuous sucrose gradient centrifugation can detach such CDs from sperm flagella [31], TAG were found to be their main lipid constituents (Supplemental Figure S2). The quantity of CD-associated TAG was equivalent to the amount of TAG that had been lost from the gametes. The fatty acid composition of CD-associated and intact sperm TAG was similar, the main PUFA of these TAG being linoleic (18:2n-6) acid (Supplemental Figure S3). These observations allowed us to conclude that most of the TAG present in our samples, confined in the small CDs, belonged to the gametes. Although sperm proteomics is a relatively recent field (see [32] for a review), this approach continues to shed light on some of the mechanisms regulating sperm metabolism and functions. Proteomic analyses of CD purified from epididymal mouse sperm showed that most of their proteins are enzymes involved in energy metabolism, supporting the idea that CD may serve a role as an energy source during epididymal sperm maturation [33]. Our observations that such particles contain most of the TAG of epididymal rat sperm, and that they remained unaffected after completion of two extra-epididymal sperm functions, Cap and AR (Supplemental Figure S4), are consistent with this interpretation.

The changes affecting rat sperm phospholipid levels after Cap and AR are essentially in agreement with findings in previous work [9]. Here we extend these results by revealing that the GPL subclasses mostly responsible for the decrease in lipid phosphorus occurring between C3 and Cap samples are the 1,2-diacyl- (PC and PE), rather than the corresponding plasmalogens, resulting in a significant change in the sperm membrane lipid composition after Cap: as the percentage of plasmenylethanolamine and plasmenylcholine increased, the latter became a major GPL.

In incubated C3 samples, hydrolysis of PE and PC could only partly explain the increase in FFA, quite superior to that of the lysophospholipids, whose levels also increased. Intriguingly, such FFAs were mostly saturates (16:0, 18:0) and 18:1. Having excluded TAG hydrolysis as its cause, the FFA accumulation in C3 suggests the occurrence of another, as yet unidentified, origin of these metabolites. Long-chain fatty acid:CoASH ligase, which couples FFA to CoASH at the expense of Mg-ATP hydrolysis, has a strict specificity for saturated fatty acids in spermatozoa, displaying peak activity with 16:0 [34]. The incubation time in C3 may have been long enough to deplete ATP levels, thereby disturbing the activity of this enzyme.

Capacitation is a highly energy-dependent process as it involves hyperactive motility and substantial levels of protein phosphorylation. In our Cap spermatozoa, the saturated FFA did not accumulate. The presence of Ca^{2+} in the medium apparently stimulated a form of phospholipase, as PC and PE in Cap samples were hydrolyzed with respect to C3 controls. However, most of the resulting FFA and corresponding lysophospholipids did not remain in the cells but were displaced to the BSA-containing medium, together with cholesterol [9]. Thus, there were less FFA available in Cap samples than in C3 controls, raising the possibility that part of the FFA was converted into acyl CoAs and metabolized. Although not tested, and taking into account that ejaculated mammalian sperms mostly depend on glycolytic processes whereas epididymal sperms mainly employ L-carnitine-dependent mitochondrial fatty acid oxidation for their energy metabolism [35], the possibility cannot be discarded that the present samples possess some degree of capacity to oxidize fatty acids. Remarkably, even in ejaculated human [36] and stallion [37] sperm, a large proportion of the metabolic proteome is comprised of enzymes involved in the mitochondrial β -oxidation of fatty acids. This metabolic pathway appears to be functional and not merely a vestige from previous sperm developmental stages.

A correlation was found between the biophysical changes detected by measuring GP values with Laurdan and the biochemical changes undergone by sperm lipid classes. Two lipid metabolites contributing to the increased GP values were FFA and Cer. In the C2 condition, despite the subtle level of the increases, they were reflected in significantly increased GP values with respect to C1 samples. The importance of FFA and Cer in reducing the (typically high) lipid *disorder* of the sperm membrane was manifested in C3 and AR samples, where the maximum amounts per sperm of FFA and Cer, respectively, concurred with the highest recorded values of GP. Laurdan detected this feature both in protein-free sperm membrane models (Figs. 6 and 7) and in entire spermatozoa (Fig. 8).

In the C3 condition, the considerable increase with respect to C2 in Laurdan GP values may be largely ascribed to the observed accumulation of FFA. This is supported by the finding that a mixture of FFA prepared to imitate the composition of the C3 FFA resulted in increased GP values when added exogenously to a liposome preparation containing the membrane lipid of fresh spermatozoa (Fig. 7). This is in agreement with previous observations in acetylcholine receptor-rich native membranes [38], where FFA like 16:0 and 18:0 (but not a PUFA like 20:4 n-6) increased Laurdan GP values.

Under Cap conditions, the significant decrease in GP values with respect to their (C3) controls may be attributed in part to the efflux of cholesterol that is a hallmark of this condition [8], but also in part to the fact that Cap cells did not accumulate saturated FFA as C3 cells did.

After completion of the AR, as in A23187-treated samples, the significant increase in Cer levels at the expense of SM is the main factor explaining the highest GP values detected by Laurdan. In addition, the percentage of acrosome-reacted spermatozoa and the Cer/SM ratios in the samples increased gradually in the same C1→C2→C3→Cap→AR order:

The fact that the magnitude of GP changes was larger in our protein-free model membranes (Fig. 6) than in actual spermatozoa (Fig. 7) is not surprising, considering the differences in shape and molecular complexity of each system. In gametes, the mere presence of membrane proteins works against the free mobility of the probe, as confirmed by comparing GP values at 360 and 290 nm (Fig. 7): the closer the sperm lipid to the membrane proteins, the greater the restriction to lipid mobility. Secondly, our protein-free liposomes contained lipid in mixed form from components of all sperm membranes, including internal ones, whereas in whole gametes only the lipids on the sperm surface were sensed by Laurdan. Thirdly, in liposomes the lipid class distribution on the surface is homogeneous, whereas on the surface of spermatozoa it is highly regionalized. The lateral diffusibility of fluorescent lipid analogs over the plasma membrane of ram and mouse sperm is faster on the flagellum than on the head [39]. Fourthly, calcium ions were not present in the medium of liposomes, but had influxed to different extents into sperm cells subjected to the five conditions of this study. These ions may themselves have contributed to increases in the membrane lipid order in whole

gametes, as previously shown in erythrocytes in calcium-containing media treated with different ionophores [40]. Lastly, the much sharper GP drop observed in Cap sperm cells than in the corresponding liposomes could be explained by Cap altering the protein-driven *transbilayer* distribution of lipids. In boar sperm, Cap very markedly activates the outward translocation of GPL and SM, a change that results in increased membrane lipid disorder, as detected by merocyanine 540 [41].

In the case of C3 samples, in addition to FFA, other lipid metabolites such as lysophospholipids or diglycerides may have contributed to the high GP values. In the case of AR samples, in addition to Cer, even the A23187 ionophore used to induce this reaction could have contributed in part to the AR-associated GP increases measured, considering that i) a small proportion of it was incorporated during incubations and remained in the membrane lipid (Fig. 2 A) and ii) increasing amounts of this ionophore, in linear form up to a certain proportion, increased the GP values when added to liposomes of dimyristoyl PC (Supplemental Figure S5). However, this observation does not preclude the contribution of FFA and Cer to the increase in GP values, which were observed when these lipids were present, whether separately or jointly, in the absence of the ionophore (Fig. 7).

Although in total lipid from whole rat spermatozoa the *proportion* of SM represents almost 10% of the phospholipids, in that of the minute heads of rat sperm it is practically twice as high, almost 20% [7]. It is therefore not unreasonable to speculate that up to 20% of Cer is locally formed on the head surface after completion of the AR. Based on this assumption it was initially perplexing to us that raising the Cer levels from 1% to 10% tended to increase the GP values in our model of sperm membrane but then doubling them to 20% tended to reduce the values (Fig. 7). However, in SM-containing systems in which the Cer/SM ratio is progressively increased by the activity of a sphingomyelinase, the formation of Cer promotes discontinuous changes in bilayer properties as Cer molecules spontaneously associate to form Cer-enriched microdomains which fuse to form large Cer-rich membrane platforms with increasing Cer concentrations [42]. These Cer structures segregate from the bulk of the liquid-crystalline fluid phase, exhibiting gel-like properties whose characteristics depend not only on the amount but also on the acyl chain length and unsaturation of the generated Cer [43]. In our case, at high Cer concentrations, Laurdan molecules may have tended to be laterally excluded from the relatively more compact Cer-rich domains to be displaced into the (more mobile or disordered) domains of PUFA-rich GPL present in the rest of the bilayers, this displacement explaining the decreased GP values.

The biophysical properties of the (n-V and h-V) SM species typically present in rat sperm head have been compared with those of better-known and more ubiquitous SM species in mammalian tissues such as 16:0 SM [44]. When probed with Laurdan, bilayers of n-V SM or h-V SM exhibit very low GP values at physiological temperatures. Both types of SM have much lower phase transition temperatures than the nearly 40 °C typical of 16:0 SM. When placed in giant unilamellar vesicles (GUVs) containing POPC, SM and cholesterol, these SM species do not tend to form laterally segregated SM-cholesterol domains as 16:0 SM typically does [44].

When organized in monolayers, n-V SM and h-V SM species occupy large mean molecular areas [45]. They tend to form films with quite loose packing densities and, despite their unusually long fatty acids, with similar thicknesses to 16:0, 18:1, or 24:1 SM species when they are in the same (liquid-expanded) phase [45], suggesting bending and partial hydration of their fatty acyl moieties. In comparison, in liquid-expanded phases, monolayers of n-V Cer and h-V Cer species show much larger mean molecular areas and larger molecular dipole moments than the corresponding SM species [46]. The estimated phase transitions of these Cer occur close to physiological temperatures, i.e., far higher than those of their n-V SM or h-V SM counterparts, but much lower than those of 16:0 Cer or 24:1 Cer species. Under the activity of a sphingomyelinase, as one of these SMs (h-28:4 SM) in the liquid-expanded state is converted into h-28:4 Cer, the hydrolytic reaction proceeds with the nucleation (and growth) of Cer-enriched condensed domains that separate from the fluid SM phase [45]. Such domains appear to be round-shaped throughout the process in contrast with the star-like shape of the 16:0 Cer domains generated from 16:0 SM [47] in similar conditions.

In their physiological location over the sperm head, the not overly compact organization of VLCPUFA-containing SM may physically facilitate the accessibility of their polar headgroups to the active site of an endogenous, membrane-located sphingomyelinase to a greater extent than if they were more compactly organized, as saturated SM are. This enzyme could be the one inadvertently (spontaneously) activated as sperm are exposed for different periods to media containing variable amounts of divalent ions, in part determining the “spontaneous” generation of Cer we observed during

sperm isolation and incubations. As the SM→Cer reaction is irreversible in spermatozoa, the high reactivity of this conversion in rat sperm could explain the high vulnerability of the acrosome exhibited by these gametes.

One of the most striking features of acrosomal exocytosis is the fusion of parts of the outer acrosomal membrane with the overlying plasma membrane. The space between these membranes swells, the membrane becomes vesiculated, and small vesicles are formed that are released to the medium in the form of *hybrid vesicle* [48]. A comparison of the lipid composition of the plasma membrane and the hybrid vesicles lost from boar spermatozoa after A23187-induced AR showed that both have the same PL/cholesterol mole ratio but that the vesicles are relatively enriched in SM, EGP and CGP, in that order, whereas in the remaining plasma membrane the order is the opposite [49]. This suggests that Cer levels in membrane and vesicles may differ. The majority of A23187-treated monkey spermatozoa retain this vesiculated acrosomal cap or "shroud" after completion of the AR [50]. Vigorous pipetting is required to remove the hybrid vesicles from these shrouds and even then, only about half the spermatozoa release their hybrid vesicles to the medium. Notably, the same acrosome-reacted sperms readily release such vesicles in the presence of oocytes or of certain oocyte-specific proteins. In our present case of A23187-treated rat sperm, most of the original SM was converted into Cer, but most of both lipids remained associated with the cells, suggesting that any vesicles formed were not released to the medium under the present *in vitro* conditions. Taken together, these observations lead us to speculate that after completion of the AR in the presence of an oocyte, spermatozoa rid themselves of their SM-rich hybrid vesicles, leaving the remaining surface membrane poor in SM but rich in the fusogenic lipid Cer.

REFERENCES

- [1] Beckman JK, Gray ME, Coniglio JG. The lipid composition of isolated rat spermatids and spermatocytes. *Biochim Biophys Acta* 1978; 530: 367-374.
- [2] Avelaño MI, Rotstein NP, Vermouth NT. Lipid remodelling during epididymal maturation of rat spermatozoa. Enrichment in plasmalogen lipids containing long-chain polyenoic fatty acids of the n-9 series. *Biochem J* 1992; 283 (Pt 1): 235-241.
- [3] Robinson BS, Johnson DW, Poulos A. Novel molecular species of sphingomyelin containing 2-hydroxylated polyenoic very-long-chain fatty acids in mammalian testes and spermatozoa. *J Biol Chem* 1992; 267: 1746-1751.
- [4] Oresti GM, Reyes JG, Luquez JM, Osses N, Furland NE, Avelaño MI. Differentiation-related changes in lipid classes with long-chain and very long-chain polyenoic fatty acids in rat spermatogenic cells. *J Lipid Res* 2010; 51: 2909-2921.
- [5] Zanetti SR, de Los Angeles MM, Rensetti DE, Fornes MW, Avelaño MI. Ceramides with 2-hydroxylated, very long-chain polyenoic fatty acids in rodents: From testis to fertilization-competent spermatozoa. *Biochimie* 2010; 92: 1778-1786.
- [6] Furland NE, Oresti GM, Antollini SS, Venturino A, Maldonado EN, Avelaño MI. Very long-chain polyunsaturated fatty acids are the major acyl groups of sphingomyelins and ceramides in the head of mammalian spermatozoa. *J Biol Chem* 2007; 282: 18151-18161.
- [7] Oresti GM, Luquez JM, Furland NE, Avelaño MI. Uneven distribution of ceramides, sphingomyelins and glycerophospholipids between heads and tails of rat spermatozoa. *Lipids* 2011; 46: 1081-1090.
- [8] Travis AJ, Kopf GS. The role of cholesterol efflux in regulating the fertilization potential of mammalian spermatozoa. *J Clin Invest* 2002; 110: 731-736.
- [9] Zanetti SR, Monclus ML, Rensetti DE, Fornes MW, Avelaño MI. Differential involvement of rat sperm choline glycerophospholipids and sphingomyelin in capacitation and the acrosomal reaction. *Biochimie* 2010; 92: 1886-1894.
- [10] Parasassi T, De SG, d'Ubaldo A, Gratton E. Phase fluctuation in phospholipid membranes revealed by Laurdan fluorescence. *Biophys J* 1990; 57: 1179-1186.
- [11] Parasassi T, Gratton E, Yu WM, Wilson P, Levi M. Two-photon fluorescence microscopy of lauridan generalized polarization domains in model and natural membranes. *Biophys J* 1997; 72: 2413-2429.
- [12] Baker MA, Smith ND, Hetherington L, Taubman K, Graham ME, Robinson PJ, Aitken RJ. Label-free quantitation of phosphopeptide changes during rat sperm capacitation. *J Proteome Res* 2010; 9: 718-729.
- [13] Varisli O, Uguz C, Agca C, Agca Y. Various physical stress factors on rat sperm motility, integrity of acrosome, and plasma membrane. *J Androl* 2009; 30: 75-86.
- [14] BLIGH EG, DYER WJ. A rapid method of total lipid extraction and purification. *Can J Biochem Physiol* 1959; 37: 911-917.
- [15] Rouser G, Fkeischer S, Yamamoto A. Two dimensional thin layer chromatographic separation of polar lipids and determination of phospholipids by phosphorus analysis of spots. *Lipids* 1970; 5: 494-496.
- [16] Visconti PE, Bailey JL, Moore GD, Pan D, Olds-Clarke P, Kopf GS. Capacitation of mouse spermatozoa. I. Correlation between the capacitation state and protein tyrosine phosphorylation. *Development* 1995; 121: 1129-1137.
- [17] Laemmli UK. Cleavage of structural proteins during the assembly of the head of bacteriophage T4. *Nature* 1970; 227: 680-685.

- [18] Larson JL, Miller DJ. Simple histochemical stain for acrosomes on sperm from several species. *Mol Reprod Dev* 1999; 52: 445-449.
- [19] Bendahmane M, Zeng HT, Tulsiani DR. Assessment of acrosomal status in rat spermatozoa: studies on carbohydrate and non-carbohydrate agonists. *Arch Biochem Biophys* 2002; 404: 38-47.
- [20] Holub BJ, Skeaff CM. Nutritional regulation of cellular phosphatidylinositol. *Methods Enzymol* 1987; 141: 234-244.
- [21] Furland NE, Zanetti SR, Oresti GM, Maldonado EN, Aveldaño MI. Ceramides and sphingomyelins with high proportions of very long-chain polyunsaturated fatty acids in mammalian germ cells. *J Biol Chem* 2007.
- [22] Palleschi S, Silvestroni L. Laurdan fluorescence spectroscopy reveals a single liquid-crystalline lipid phase and lack of thermotropic phase transitions in the plasma membrane of living human sperm. *Biochim Biophys Acta* 1996; 1279: 197-202.
- [23] Buffone MG, Verstraeten SV, Calamera JC, Doncel GF. High cholesterol content and decreased membrane fluidity in human spermatozoa are associated with protein tyrosine phosphorylation and functional deficiencies. *J Androl* 2009; 30: 552-558.
- [24] Buffone MG, Doncel GF, Calamera JC, Verstraeten SV. Capacitation-associated changes in membrane fluidity in asthenozoospermic human spermatozoa. *Int J Androl* 2009; 32: 360-375.
- [25] Visconti PE, Stewart-Savage J, Blasco A, Battaglia L, Miranda P, Kopf GS, Tezon JG. Roles of bicarbonate, cAMP, and protein tyrosine phosphorylation on capacitation and the spontaneous acrosome reaction of hamster sperm. *Biol Reprod* 1999; 61: 76-84.
- [26] Nixon B, MacIntyre DA, Mitchell LA, Gibbs GM, O'Bryan M, Aitken RJ. The identification of mouse sperm-surface-associated proteins and characterization of their ability to act as decapacitation factors. *Biol Reprod* 2006; 74: 275-287.
- [27] Leahy T, Gadella BM. Sperm surface changes and physiological consequences induced by sperm handling and storage. *Reproduction* 2011; 142: 759-778.
- [28] Varisli O, Uguz C, Agca C, Agca Y. Effect of chilling on the motility and acrosomal integrity of rat sperm in the presence of various extenders. *J Am Assoc Lab Anim Sci* 2009; 48: 499-505.
- [29] Varisli O, Scott H, Agca C, Agca Y. The effects of cooling rates and type of freezing extenders on cryosurvival of rat sperm. *Cryobiology* 2013; 67: 109-116.
- [30] Harper CV, Cummerson JA, White MR, Publicover SJ, Johnson PM. Dynamic resolution of acrosomal exocytosis in human sperm. *J Cell Sci* 2008; 121: 2130-2135.
- [31] Garbers DL, Wakabayashi T, Reed PW. Enzyme profile of the cytoplasmic droplet from bovine epididymal spermatozoa. *Biol Reprod* 1970; 3: 327-337.
- [32] Brewis IA, Gadella BM. Sperm surface proteomics: from protein lists to biological function. *Mol Hum Reprod* 2010; 16: 68-79.
- [33] Yuan S, Zheng H, Zheng Z, Yan W. Proteomic analyses reveal a role of cytoplasmic droplets as an energy source during epididymal sperm maturation. *PLoS One* 2013; 8: e77466.
- [34] Jones RE, Plymate SR. Kinetics of human spermatozoa long-chain fatty acid: CoASH ligase. *J Androl* 1986; 7: 323-327.
- [35] Lenzi A, Lombardo F, Gandini L, Dondero F. [Metabolism and action of L-carnitine: its possible role in sperm tail function]. *Arch Ital Urol Nefrol Androl* 1992; 64: 187-196.
- [36] Amaral A, Castillo J, Estanyol JM, Balleca JL, Ramalho-Santos J, Oliva R. Human sperm tail proteome suggests new endogenous metabolic pathways. *Mol Cell Proteomics* 2013; 12: 330-342.
- [37] Swegen A, Curry BJ, Gibb Z, Lambourne SR, Smith ND, Aitken RJ. Investigation of the stallion sperm proteome by mass spectrometry. *Reproduction* 2015; 149: 235-244.
- [38] Antollini SS, Barrantes FJ. Unique effects of different fatty acid species on the physical properties of the torpedo acetylcholine receptor membrane. *J Biol Chem* 2002; 277: 1249-1254.
- [39] Wolf DE, Hagopian SS, Ishijima S. Changes in sperm plasma membrane lipid diffusibility after hyperactivation during in vitro capacitation in the mouse. *J Cell Biol* 1986; 102: 1372-1377.
- [40] Vest RS, Gonzales LJ, Permann SA, Spencer E, Hansen LD, Judd AM, Bell JD. Divalent cations increase lipid order in erythrocytes and susceptibility to secretory phospholipase A2. *Biophys J* 2004; 86: 2251-2260.
- [41] Gadella BM, Harrison RA. The capacitating agent bicarbonate induces protein kinase A-dependent changes in phospholipid transbilayer behavior in the sperm plasma membrane. *Development* 2000; 127: 2407-2420.
- [42] Bollinger CR, Teichgraber V, Gulbins E. Ceramide-enriched membrane domains. *Biochim Biophys Acta* 2005; 1746: 284-294.
- [43] Pinto SN, Laviad EL, Stiban J, Kelly SL, Merrill AH, Jr., Prieto M, Futerman AH, Silva LC. Changes in membrane biophysical properties induced by sphingomyelinase depend on the sphingolipid N-acyl chain. *J Lipid Res* 2014; 55: 53-61.
- [44] Peñalva DA, Furland NE, Lopez GH, Aveldaño MI, Antollini SS. Unique thermal behavior of sphingomyelin species with nonhydroxy and 2-hydroxy very-long-chain (C28-C32) PUFAs. *J Lipid Res* 2013; 54: 2225-2235.
- [45] Peñalva DA, Wilke N, Maggio B, Aveldaño MI, Fanani ML. Surface behavior of sphingomyelins with very long chain polyunsaturated fatty acids and effects of their conversion to ceramides. *Langmuir* 2014; 30: 4385-4395.
- [46] Peñalva DA, Oresti GM, Dupuy F, Antollini SS, Maggio B, Aveldaño MI, Fanani ML. Atypical surface behavior of ceramides with nonhydroxy and 2-hydroxy very long-chain (C28-C32) PUFAs. *Biochim Biophys Acta* 2014; 1838: 731-738.
- [47] Fanani ML, Hartel S, Maggio B, De TL, Jara J, Olmos F, Oliveira RG. The action of sphingomyelinase in lipid monolayers as revealed by microscopic image analysis. *Biochim Biophys Acta* 2010; 1798: 1309-1323.
- [48] Zanetti N, Mayorga LS. Acrosomal swelling and membrane docking are required for hybrid vesicle formation during the human sperm acrosome reaction. *Biol Reprod* 2009; 81: 396-405.
- [49] Nikolopoulou M, Soucek DA, Vary JC. Lipid composition of the membrane released after an in vitro acrosome reaction of epididymal boar sperm. *Lipids* 1986; 21: 566-570.
- [50] VandeVoort CA, Yudin AI, Overstreet JW. Interaction of acrosome-reacted macaque sperm with the macaque zona pellucida. *Biol Reprod* 1997; 56: 1307-1316.

FIGURE LEGENDS

Figure 1: Evaluation of membrane integrity, tyrosine protein phosphorylation and acrosomal status of rat spermatozoa after isolation and functional activation. C1, sperm isolated from the epididymis in the presence of EDTA; C2, sperm isolated similarly but in the absence of this chelator; C3, Cap, and AR, spermatozoa isolated as in C2 and then incubated for the same period (5.5 h) and in the same medium, as follows: C3, with no additions; Cap, in the presence of Ca^{2+} , HCO_3^- and BSA to induce capacitation; and AR, sperm incubated in the same conditions as in Cap, but exposed to A23147 during the last 30 min to induce the acrosomal reaction. Viability was assessed using Hoechst 33342 to locate the cells by staining their nuclei, and propidium iodide (PI) to locate cells with a compromised membrane; in A) representative phase and fluorescence microscopy images of the same field are shown and in B) the percentage of viable cells was quantified. The amounts of spermatozoa that had undergone the acrosomal reaction after each of the described treatments, as evaluated with Coomassie brilliant blue, is shown in C). Results in B and C are mean values \pm SD of 4 independent experiments. NS, not significant differences; asterisks indicate statistical significant differences with respect to C1, ($P < 0.05$, Student t-test). Panel D) illustrates a representative immunoblot showing the tyrosine-phosphorylated proteins produced after each of the conditions or treatments, probed as described in *Materials and Methods*.

Figure 2. Lipids of rat spermatozoa after isolation and functional activation *in vitro*. The conditions or treatments whose abbreviations are C1, C2, C3, Cap, and AR and the style of the bars corresponding to each of these five conditions (black, gray, white, hatched and dotted bars, respectively) are the same for Figures 2 to 5, namely: C1, sperm isolated from the epididymis in the presence of EDTA; C2, sperm isolated similarly but in the absence of this chelator; C3, Cap, and AR, spermatozoa isolated as in C2 and then incubated for the same period and in the same medium as follows: C3, with no additions; Cap, in the presence of BSA, calcium ions and bicarbonate to induce capacitation; and AR, sperm incubated in the same conditions as in Cap, but exposed to A23147 during the last 30 min to induce the acrosomal reaction. In A) a TLC plate qualitatively comparing the lipid profiles among these 5 conditions was prepared by spotting aliquots, taken from sperm lipid extracts containing a fixed amount (10 μg) of total lipid phosphorus. In B) a quantitative comparison is presented, showing the amounts contained in a fixed amount of cells (10^9) of total phospholipids (Total PL), total (diradyl) choline glycerophospholipids (CGP), ethanolamine glycerophospholipids (EGP) and sphingomyelin (SM), as determined by phosphorus analysis. The lipid abbreviations in (A) correspond to: CE, cholesterol esters; ADG, ether-linked triglycerides; TAG, triacylglycerols; CoQ, coenzyme Q; Cho, cholesterol; DAG, diacylglycerols; Cer, ceramides with nonhydroxy fatty acids; HO-Cer, ceramides with 2-hydroxy fatty acids; 1^{st} SF, first solvent front; GleCer, glucosylceramide; SL, seminolipid; CL, cardiolipin; EGP, ethanolamine glycerophospholipids; PI, phosphatidylserine; PI, phosphatidylinositol; CGP, choline glycerophospholipids; SM, sphingomyelin; LPC, lysophosphatidylcholine. The asterisk (*) points to the A23187 ionophore present in lipid extracts from AR samples.

Figure 3. Quantitative changes in lipid constituents of rat spermatozoa after isolation and activation *in vitro*. The same five abbreviations, order, and styles of the bars as defined in the legend of Fig. 2B were used. C1, sperm isolated in the presence of EDTA; C2, sperm isolated similarly but in the absence of EDTA; C3, Cap, and AR, are spermatozoa isolated as in C2 and then incubated for the same period and in the same medium with no additions (C3) or with the additions required to induce capacitation (Cap) and the acrosomal reaction (AR). Lipid abbreviations: PC and PE, phosphatidylcholine and phosphatidylethanolamine, respectively; P-PC and P-PE, plasmalogen choline and plasmalogen ethanolamine, respectively (due to space restrictions, the prefix P- was used in this figure as an abbreviation of these two plasmalogens, as they contain an alk-1-enyl-bound fatty aldehyde (instead of an ester-bound fatty acid), in *sn*-1; CL, cardiolipin; PA, phosphatidic acid; PS and PI, phosphatidyl- serine and inositol, respectively; DAG, diacylglycerols; LPC and LPE, lysoPC

and lysoPE, respectively; Cho, free cholesterol; FFA, free fatty acids; SM, sphingomyelins; Cer, ceramides. Asterisks denote significant differences among conditions or treatments ($P < 0.01$).

Figure 4. Variations in the amounts of representative fatty acids of major rat sperm subclasses of (diradyl) choline and ethanolamine glycerophospholipids after isolation and incubation. The abbreviations corresponding to the five conditions or treatments, their order, and styles of the bars are the same as in the previous figures: C1, sperm isolated in the presence of EDTA; C2, sperm isolated similarly but in the absence of EDTA; C3, Cap, and AR, spermatozoa isolated as in C2 and then incubated for the same period and in the same medium with no additions (C3) or with the additions required to induce capacitation (Cap) and the acrosomal reaction (AR). The CGP and EGP were separated into subclasses by TLC and their fatty acids analyzed by GC. The fatty acids are abbreviated by the convention, number of carbon atoms : number of double bonds.

Figure 5. Variations in the amounts of main groups of fatty acids of sphingomyelin (SM) and ceramide (Cer) of rat spermatozoa after isolation and incubations. The abbreviations, order, and styles of the bars are the same as in the previous figures: C1, sperm isolated in the presence of EDTA; C2, sperm isolated similarly but in the absence of EDTA; C3, Cap, and AR, spermatozoa isolated as in C2 and then incubated for the same period and in the same medium with no additions (C3) or with the additions required to induce capacitation (Cap) and the acrosomal reaction (AR). The SM and Cer were separated, their fatty acids were analyzed by GC and then grouped into saturated (S), monoenoic (M), nonhydroxy VLCPUFA (n-V) and 2-hydroxy VLCPUFA (h-V).

Figure 6. Changes in the generalized polarization (GP) of Laurdan, as a measure of lipid order, in protein-free membrane models obtained from rat spermatozoa after the five experimental conditions of this study. Liposomes were prepared in the presence of Laurdan using total lipid extracts from the samples whose components are shown in Figures 1 to 4. The GP values obtained at two temperatures are shown. The abbreviations, order, and styles of the bars for the 5 treatments are the same as in the previous figures. Different letters (a-e) denote significant differences among samples ($P < 0.01$).

Figure 7. Net variation in the generalized polarization (Δ GP) of Laurdan in a model membrane, as modified by the presence of free fatty acids (FFA) and ceramides (Cer). Liposomes were prepared from the polar lipid (PL) isolated from C1 sperm samples (hatched bar), to which 20% cholesterol (dark grey bar) and then 20% cholesterol and 0.6% Cer were added (no bar, pointed with the arrow). This combination, imitating the PL:Chol: Cer ratio present in native sperm membranes, was then used as the reference to evaluate the effects of adding to it the indicated proportions of FFA (white bars), Cer (black bars) and their combination (light grey bar). The FFA used here imitated the composition of the FFA accumulated in C3 and the Cer were isolated from AR samples. The data were obtained at 37°C and are expressed as differences (Δ) of GP values between each group and that taken as reference (arrow). Different letters (a-e) denote significant differences among samples ($P < 0.01$).

Figure 8. Net variation in the generalized polarization (Δ GP) of Laurdan in rat sperm cells, recorded at the indicated wavelengths, after the five experimental conditions and treatments under study. The abbreviations are the same as in Figures 1-5. The data were obtained at 37°C and are expressed as differences (Δ) of GP values between experimental and reference samples. In this case the GP obtained for the C1 condition was used as the reference.

Figure 1

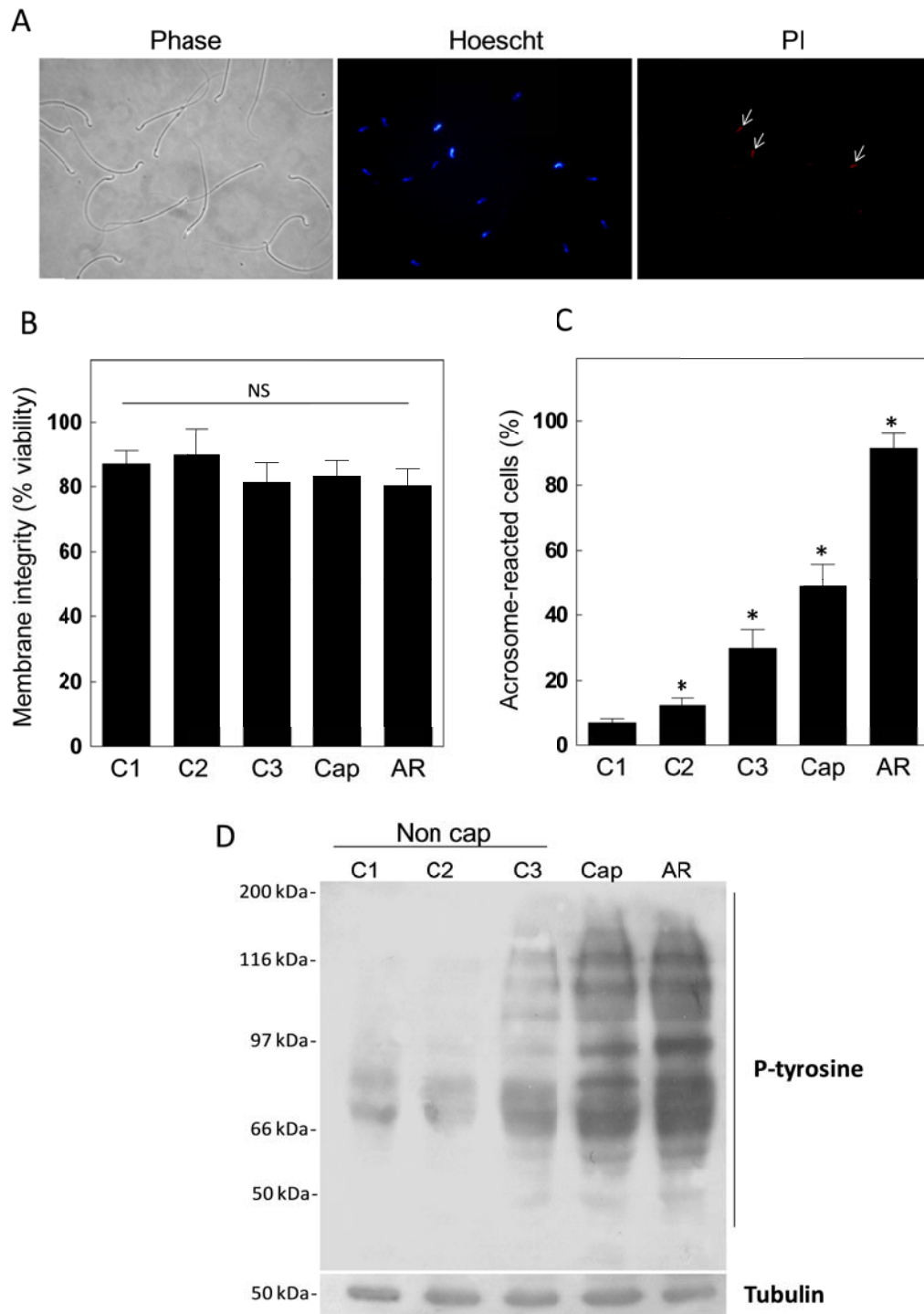


Figure 2

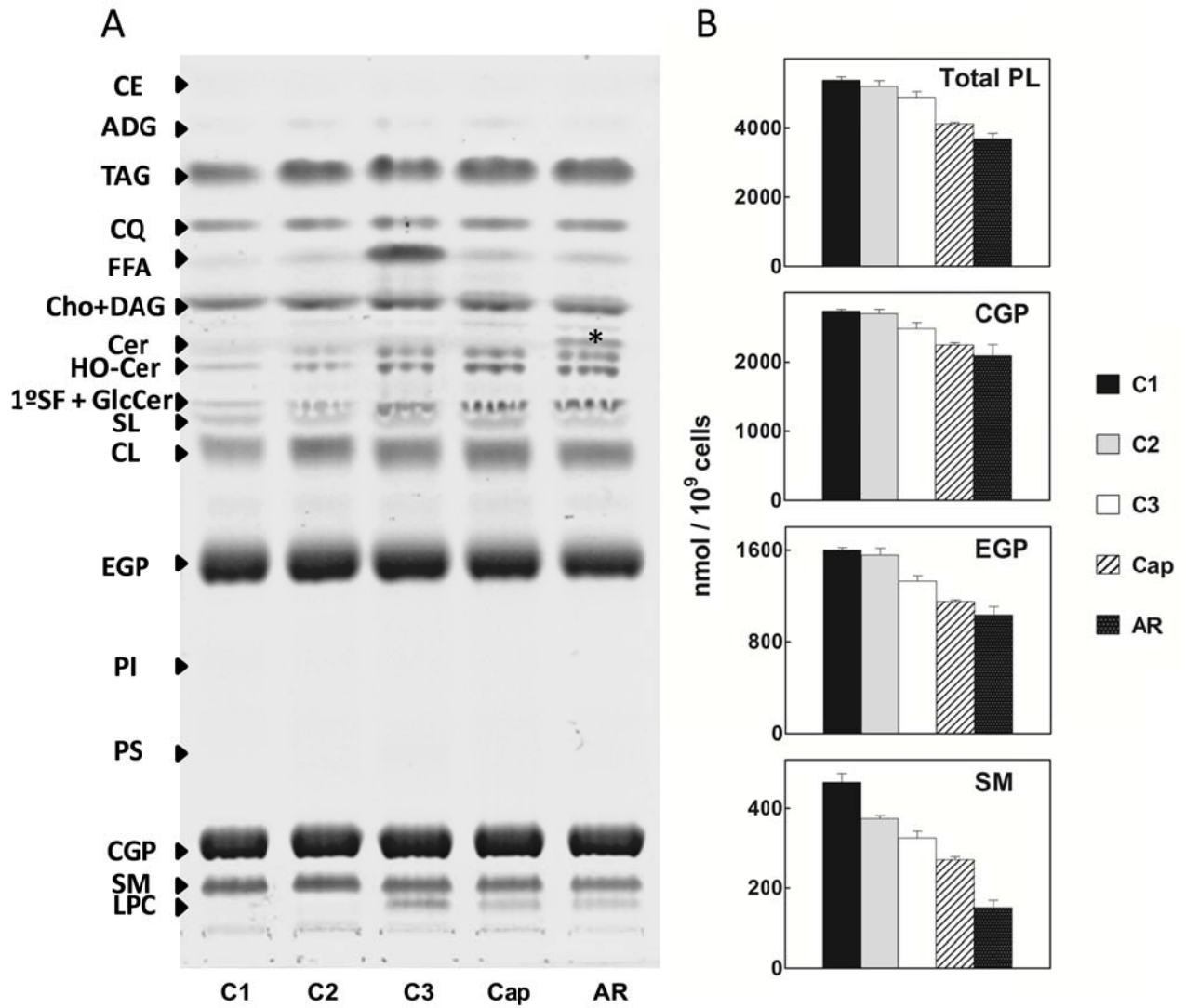


Figure 3

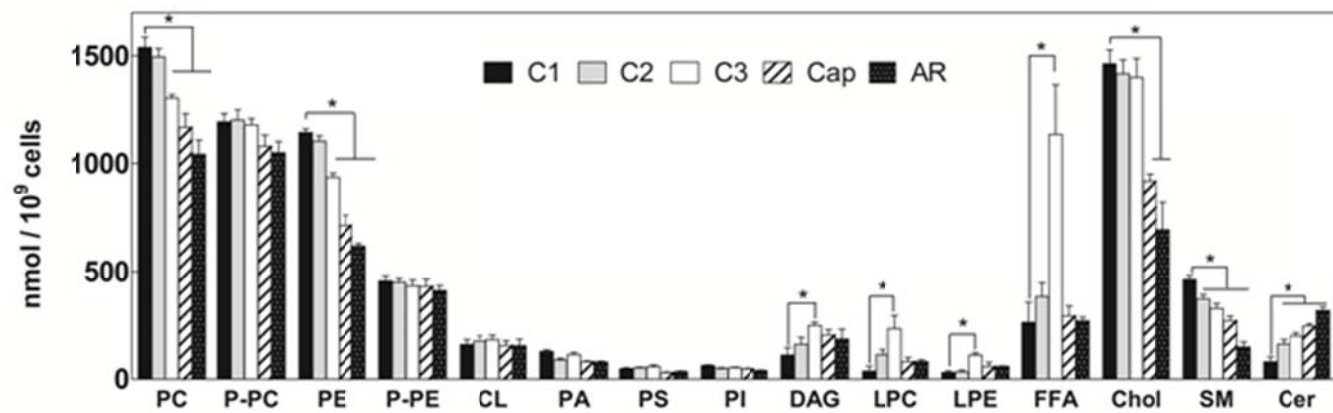


Figure 4

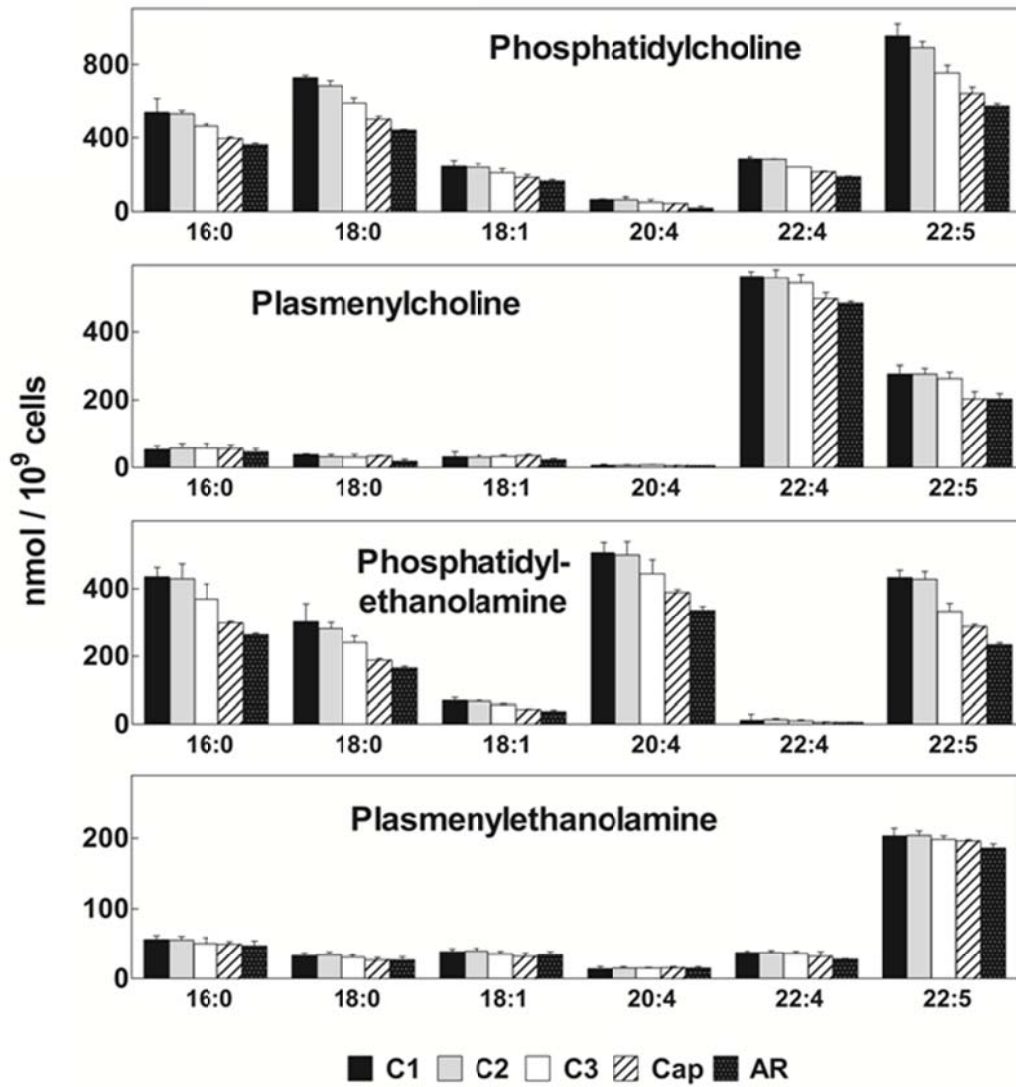


Figure 5

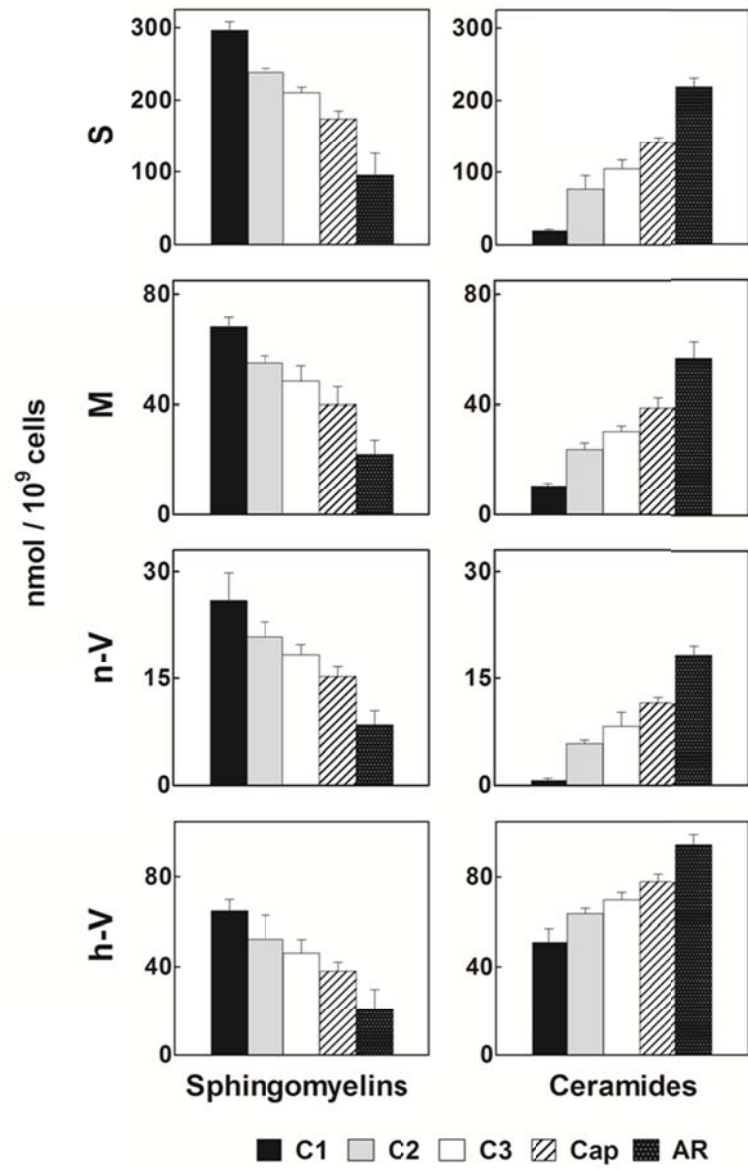


Figure 6

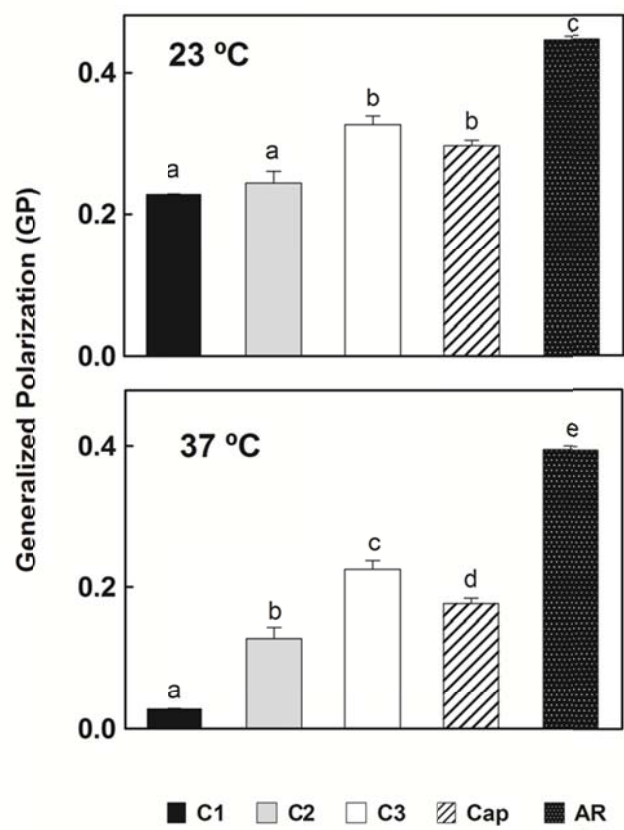


Figure 7

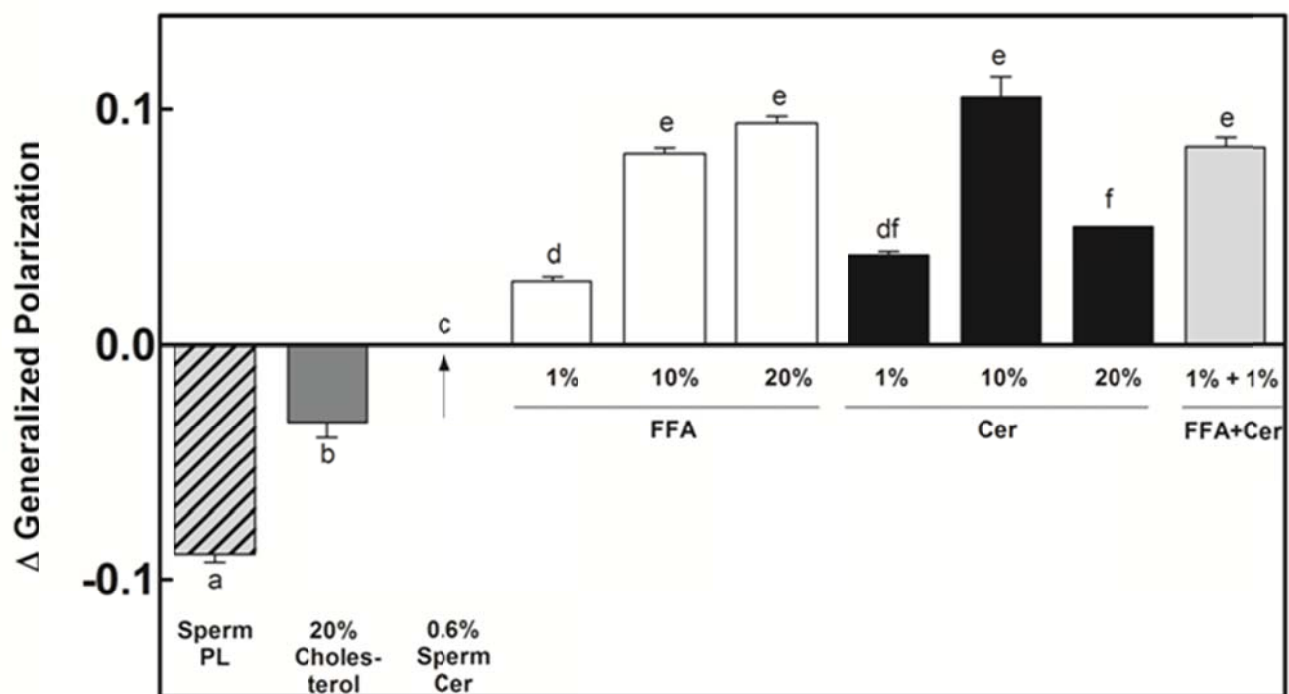


Figure 8

